CHAPTER III

RESULTS AND DISCUSSION

3.1 Tensile Testing

Figure 3.1 shows the dependence of Young's modulus upon the weight percentage of filler. The elastic modulus increases with increasing filler content. It also can be seen that the modulus does not depend on average particle size. The polymeric matrix is stiffened by the $CaCO_3$ filler. The particle restrict the mobility and deformability of the matrix by introducing a mechanical restraint. The restriction in polymer mobility in the presence of solid particles occurs due to an effective attraction potential between segments of the chain and the repulsive potential that the polymer is subjected to when it is close to the solid particles. The degree of particle restriction depends on the properties of the particle and the matrix (J. A. Manson, 1976). It is also noted that the modulus increment is greater at higher filler loadings than lower filler loadings. This is likely due to particle-particle interaction, which becomes significant at higher filler loadings.

Poor stress transfer at the filler-polymer interface is the major problem in particulate filled composite. Discontinuity is created in the structure because of nonadherence of the filler to the polymer which may give rise to dewetting. The filler particles cannot carry any load, which then act as a weak body. Stress concentrations will be created around the particles and reduce the composite strength. The important requirements for contributing mechanical properties by a dispersed phase in a two-phase composite are

continuity in the structure and interfacial adhesion. The tensile strength data will be analysed to detect these aspects of the composite.

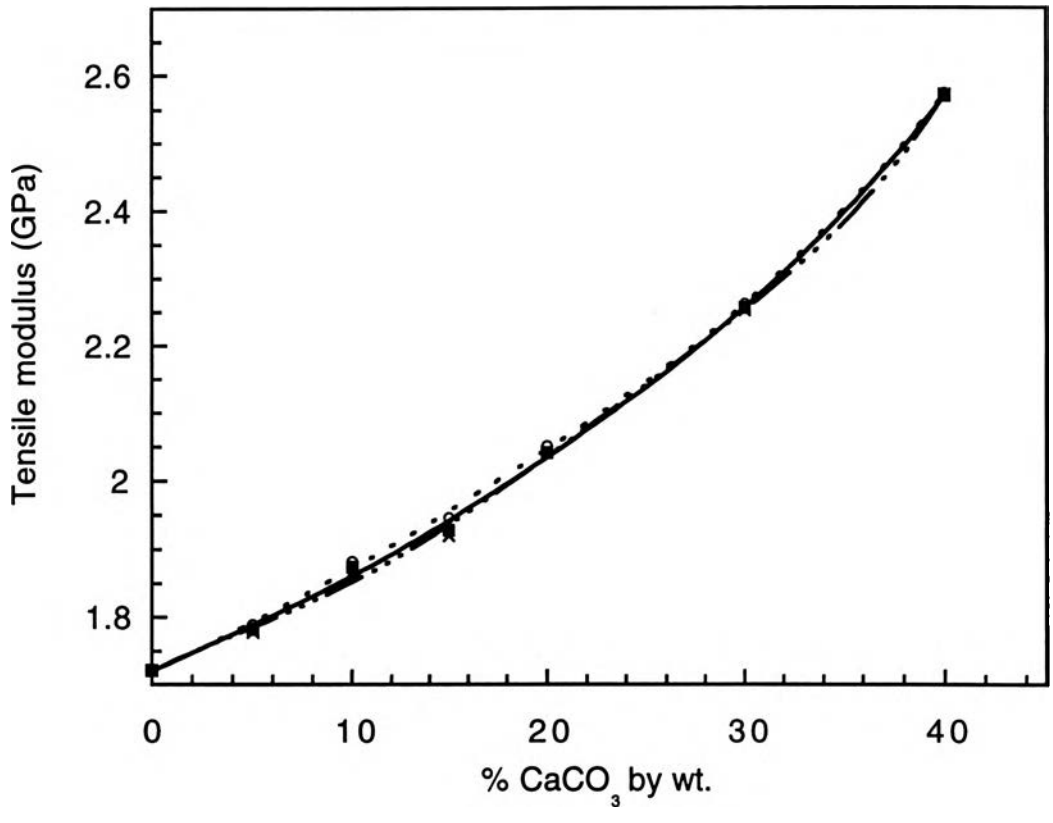

Figure 3.1 Plot of tensile modulus of B-a / untreated $CaCO_3$ against weight percentage of the filler for 1 μm (O), 5 μm (■) and 20 μm (×) average particle size.

To explore the generation of discontinuity and sequential weakness in the structure of these two-phase composites, the tensile strength was analyzed using the theoretical predictive models which are:

$$\sigma_c/\sigma_p = (1-\phi_F^{2/3})S \quad (1)$$

$$\sigma_c/\sigma_p = (1-K\phi_F^{2/3}) \quad (2)$$

where σ_c and σ_P are the tensile strength of the composite and matrix, respectively and ϕ_F is the volume fraction of the filler. The parameter S in eq.(1) account for the weakness in the structure caused by the discontinuity in stress transfer and generation of stress concentration at the filler-polymer interface, as proposed by Nielsen (L. E. Nielsen, 1966). When there is no stress concentration effect, the S value will be maximum which equals to unity. The lower the S value, the greater the stress concentration effect. The parameter K in eq.(2) is taken into account of the adhesion quality between the matrix and the filler (L. Nicolais, 1971). The lower the K value is, the better the adhesion will be.

Figure 3.2 is the plot of tensile strength against the weight percentage of $CaCO_3$. It shows the effects of particle size and surface treatment of $CaCO_3$ on the tensile strength. The tensile strength decreases with increasing filler content for all sizes of $CaCO_3$. A similar trend is observed for samples filled with surface treated $CaCO_3$. In general, tensile strength of the filled polymer increases with a decrease in the particle size. However, in the $CaCO_3$ filled B-a system, the composite of B-a / 5 μm $CaCO_3$ posseses the highest tensile strength, whereas either larger or smaller particle size shows the lower tensile strength. Furthermore, the tensile strength of polybenzoxazine filled with untreated $CaCO_3$ is higher than that of the surface treated one, which disagree with the expectation. The stearic acid modified surface of $CaCO_3$ should give the higher tensile strength due to the better dispersion. These results can be explained by using the above equation (eq 1-2). The average values of stress concentration parameter S (eq(1)), and adhesion properties K (eq(2)) in B-a / $CaCO_3$ composite are calculated, as shown in Table 3.1.

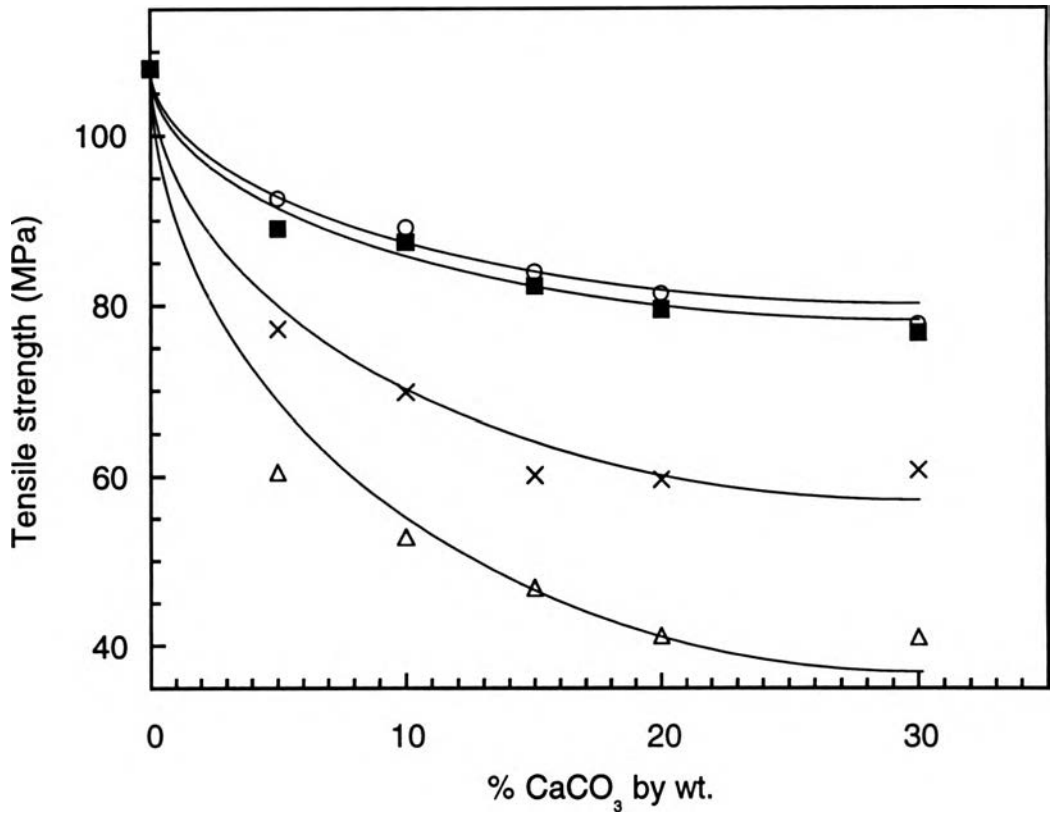

Figure 3.2 Tensile stress of B-a / $CaCO_3$ composite vs. weigth fraction for $CaCO_3$ with treated surface 5 μm (■) and untreated surface 1μm (×), 5 μm (O) and 20 μm (Δ) average particle size.

The S value of the composite filled with untreated 5 μm $CaCO_3$ is higher than that of untreated 1μm and 20 μm, indicating that the stress concentration in B-a / untreated 5 μm $CaCO_3$ is less. It is possible that the stress at which dewetting occurs depend on the size of the filler. And it may be due to an agglomeration of the untreated 1 μm to form large particles so that its tensile strength decreases to be lower than the untreated 5 μm $CaCO_3$.

Table 3.1 The S and K values of B-a filled with 30% by wt. of different typesof $CaCO_3$.

Type of $CaCO_3$	S	K
Surface treated, 5 μm	0.93	1.45
Untreated, 5 μm	0.96	1.28
Untreated, 1 μm	0.74	2.41
Untreated, 20 μm	0.56	3.51

The composite with surface-treated $CaCO_3$ shows a similar degree of stress concentration with the untreated one. However, the lower K value indicates poorer adhesion between the matrix and surface treated $CaCO_3$ (B. Pukanszky, 1988)

3.2 Flexural Testing

The results of the flexural testing mirrored those of the tensile experiments. Figure 3.3 shows the effect of particle content, particle size, and surface treatment on the flexural modulus. Flexural modulus increases with an increase in $CaCO_3$ content. And the flexural modulus of untreated $CaCO_3$ is slightly higher than the composite with surface treated $CaCO_3$.

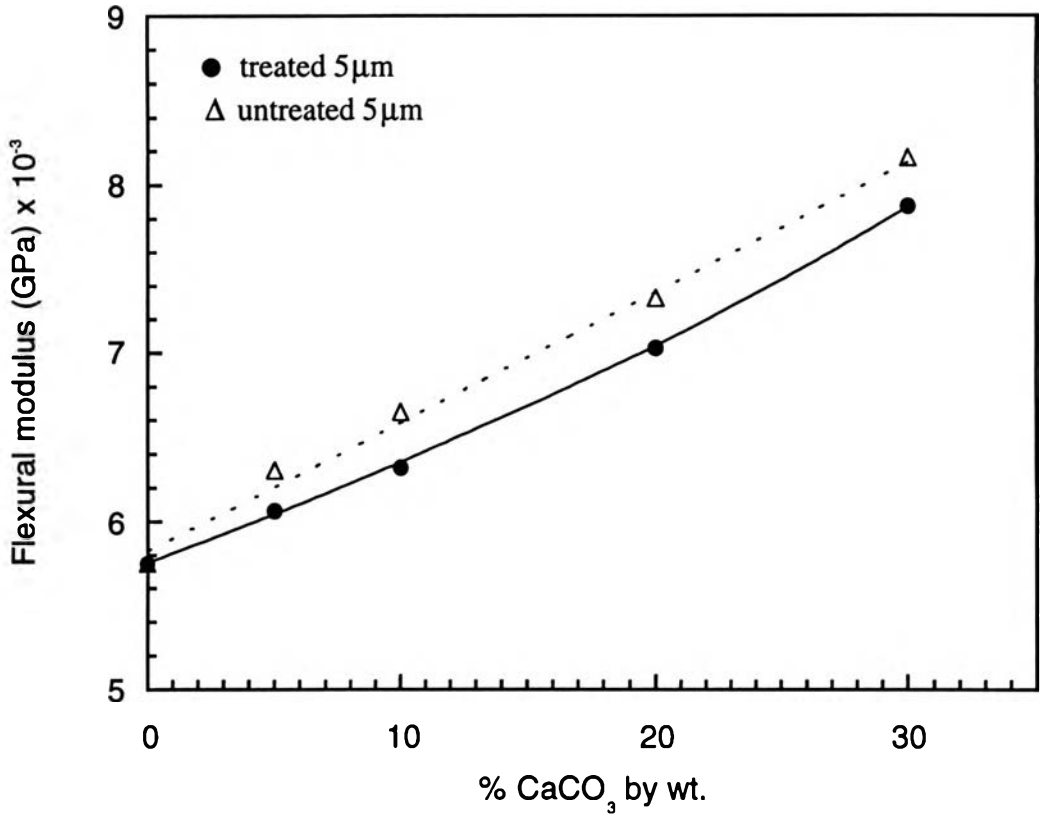

Figure 3.3 Plot of flexural modulus of B-a / 5 μm $CaCO_3$ with treated (●) and untreated (Δ) surfaces against weight percentage of $CaCO_3$.

The effect of particle content, particle size, and surface treatment on the flexural strength are shown in Figure 3.4. Flexural strength decreases with increasing filler content. The composite with surface treated $CaCO_3$ shows lower strength than that of the untreated one. Flexural strength of B-a / untreated 5 μm $CaCO_3$ is highest, whereas the smaller and larger particle size give the less value.

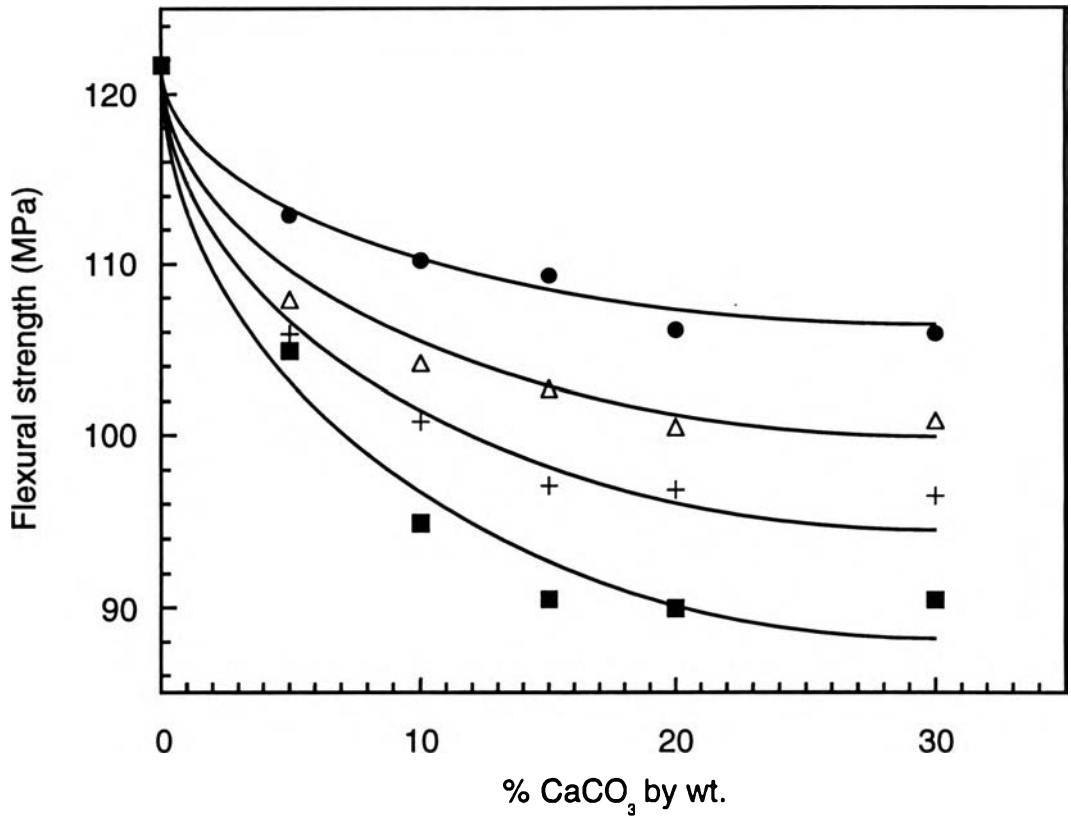

Figure 3.4 Flexural strength of B-a filled with $CaCO_3$, as a function of the weight percentage, for 5 μm surface treated $CaCO_3$ (■) and untreated $CaCO_3$ with particle sizes of 1 μm (Δ), 5 μm (●), and 20 μm (+).

The flexural strength and flexural modulus of B-a / $CaCO_3$ composite are higher than those of polyester / $CaCO_3$ and epoxy / $CaCO_3$ composite (see Table 3.2), showing that the B-a / $CaCO_3$ is much stronger and stiffer. It may be due to the B-a structure containing more aromatic rings (H. V. Baenig, 1973 and V. R. Gowariker, 1986). Aromatic rings have localised electron at π orbital and resonance effects resulting in increasing the strength and stiffness of material.

Table 3.2 The flexural strength and modulus of $CaCO_3$ filled with matrix of B-a, polyester and epoxy (M. M. Schwartz, 1984 and G. Lubin, 1982).

Matrix	wt.% $CaCO_3$	Flexural Modulus (GPa)	Flexural Strength (MPa)
B-a	23.1	7.6	106.5
Polyester	23.1	7.1	62
B-a	28.6	8.0	106
Epoxy	28.6	3.54	31.9

3.3 Izod Impact Testing

The izod impact strength values of B-a / $CaCO_3$ composites are shown in Figure 3.5 as a function of weight percentage. The dramatic drop of the impact strength is observed at small $CaCO_3$ concentrations (up to 15% by wt.). On further filling, the impact strength remains almost unchanged. The impact strength of the composite is lower than that of unfilled B-a due to the adding of $CaCO_3$ which makes composite more brittleness. The effect of $CaCO_3$ content on the impact properties of composite is similar between surface treated $CaCO_3$ and untreated $CaCO_3$. However, the composite with untreated $CaCO_3$ shows higher impact strength than the surface treated $CaCO_3$-filled composites. This is once attributed to the lubricating effect by

the stearic acid. Impact strength increases if the adhesion between the polymer and filler is increased (N. S. Enikolopyan, 1990).

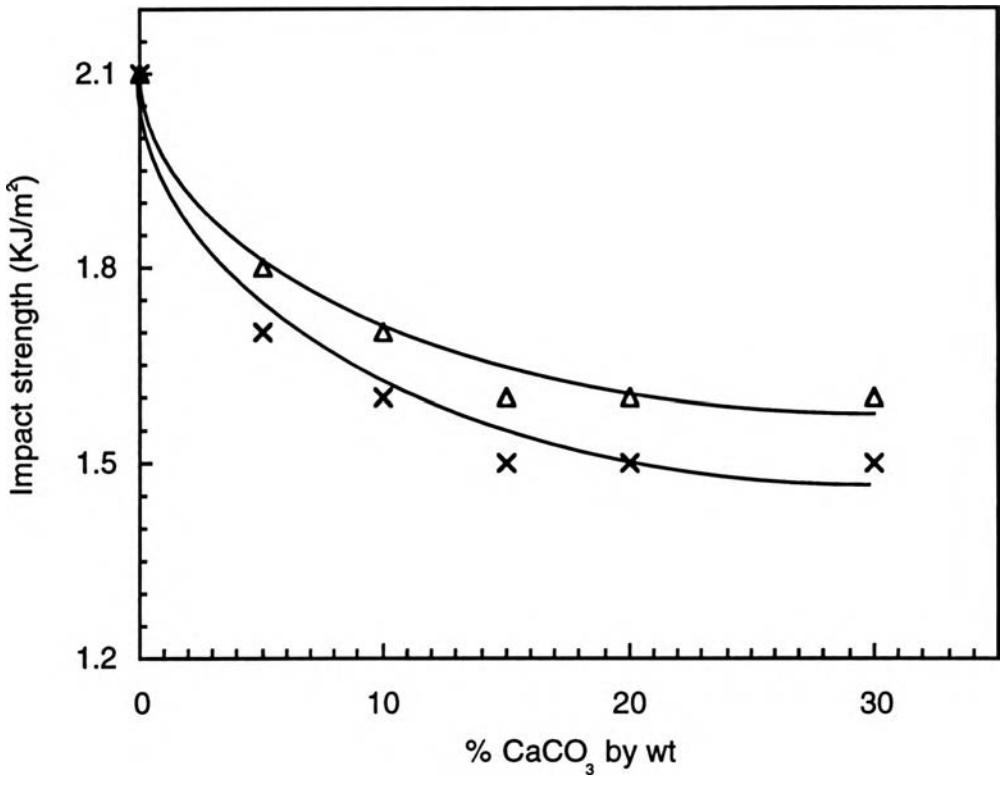

Figure 3.5. Plot of impact strength of B-a filled with $CaCO_3$, as a function of the weight percentage, for surface untreated (Δ) and treated (×) with stearic acid.

3.4 Dynamic Mechanical Measurement

In a composite material which consists of filler, a polymer matrix and a filler/matrix interface, some of the deformation energy will be dissipated, mainly in the matrix and possibly at the interface. The interface is an additional source of energy lost by any mechanism, for example heat. In a DMA test, these losses manifest themselves as an increase in the viscous response of the material. During deformation, a composite material with poor

interfacial bonding will tend to dissipate more energy than the same composite with good interfacial bonding (J. M. Kennedy,1992).

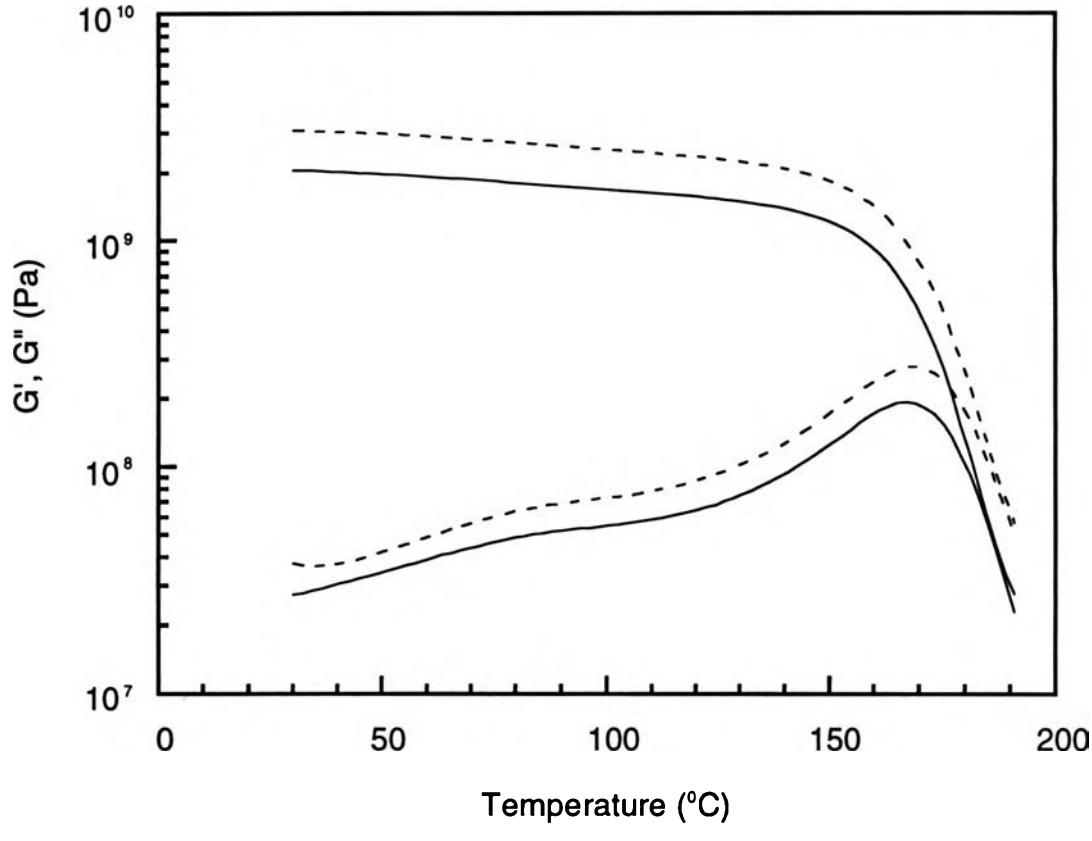

Figure 3.6 Dynamic mechanical spectra of cured unfilled B - a (——) and filled B-a with 30% $CaCO_3$ (----).

The dynamic mechanical spectra of unfilled B-a and B-a filled with 30 wt.% of $CaCO_3$ are presented in Figure 3.6. The unfilled B-a spectra shows the Tg at 167 °C, whereas the spectra of B-a filled with 30 wt.% of $CaCO_3$ displays the Tg at 169 °C, indicating that $CaCO_3$ particles restrict the mobility of chains at the glass transition temperature. However, the storage modulus, G′, and loss modulus,G″, of the B-a / 30% $CaCO_3$ are higher than those of unfilled B-a since adding the filler makes the composite more elastic. But at

the same time, the filler / matrix interface with poorer adhesion dissipates more energy resulting in increased of viscous component.

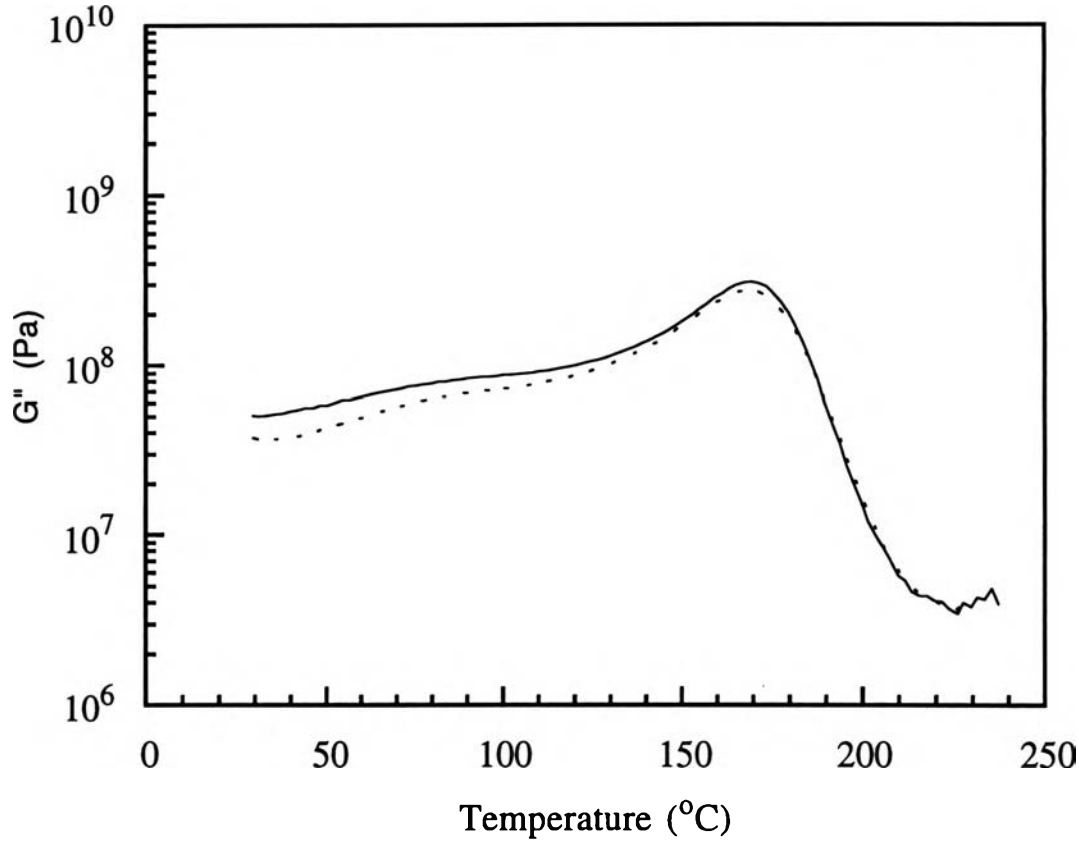

Figure 3.7 Loss modulus of filled B-a with 5 μm surface treated (—) and untreated (----) $CaCO_3$.

In Figure 3.7, G″ of the sample fabricated from surface treated $CaCO_3$ is compared to that obtained from the polymer filled with $CaCO_3$ with no surface treatment. The loss modulus of the specimen fabricated with surface treated $CaCO_3$ by 30 wt.% is higher than the sample made with the untreated $CaCO_3$, indicating that the surface treated $CaCO_3$ give poorer interfacial bonding with the matrix than the untreated $CaCO_3$. The effect of interfacial bonding also can be seen from the tan δ peak, as shown in Figure 3.8. The

lower the tan δ peak, the better the interfacial bonding. Therefore the surface treated $CaCO_3$ by stearic acid result in a higher value of tan δ.

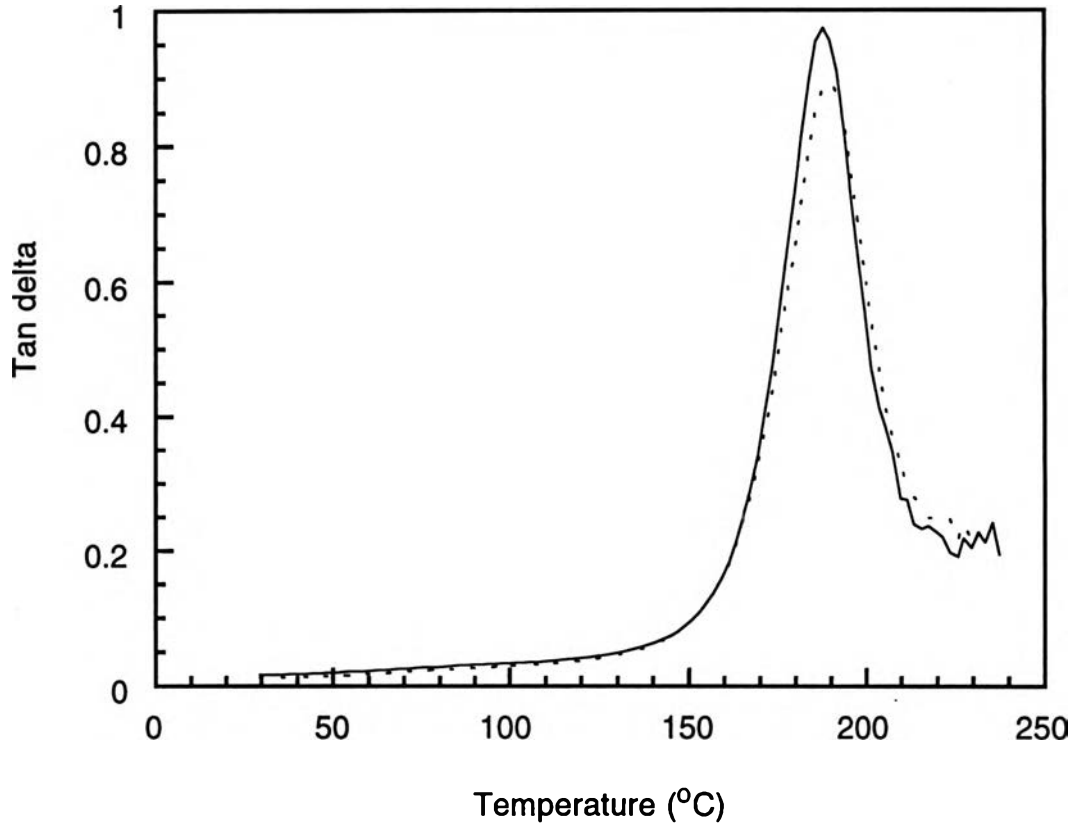

Figure 3.8 Tan δ of filled B-a with 5 μm surface treated (—) and untreated (- - -) 30 wt.% $CaCO_3$.

Figure 3.9 is the comparation of the loss moduli measured on the specimens which are made of different sizes of $CaCO_3$. The G″ of the composites slightly decreases in order of the $CaCO_3$ size 20 μm, 1 μm and 5 μm.

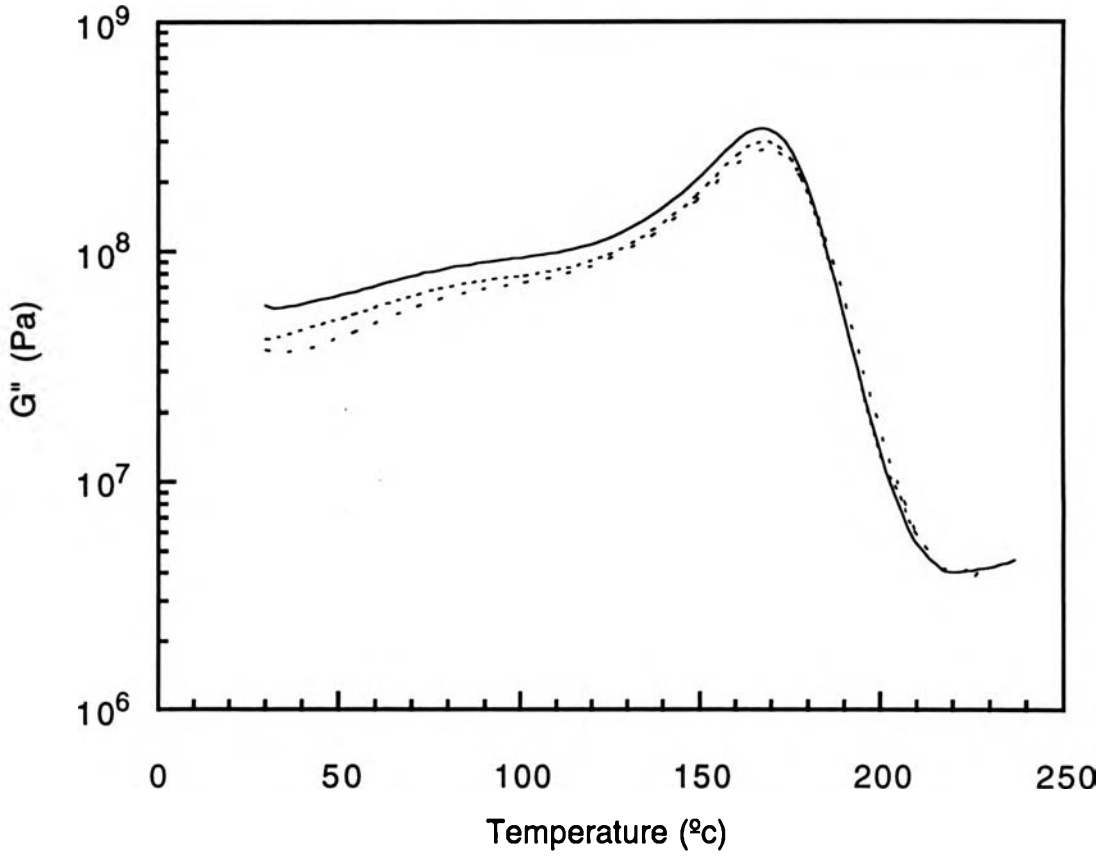

Figure 3.9 Loss modulus of filled B-a with $CaCO_3$ for particle size 1 μm (----), 5 μm (- - -), and 20 μm (—).

As the dynamic mechanical measurements are carried out in the frequency / temperature sweep mode, different Tg's are observed at various frequencies. The activation enthalpy of the glass transition process can be calculated from the following equation (Z. M. Ward, 1993):

$$ln\frac{\omega_2}{\omega_1} = \frac{\Delta H}{R}\left(\frac{1}{Tg_2} - \frac{1}{Tg_1}\right) \qquad (3)$$

where ΔH is the activation enthalpy, R is the gas contant, Tg_1 and Tg_2 are the glass transition temperatures in Kelvin and correspond to the test

frequencies, ω_1 and ω_2, respectively. The Arrhenius plots of B-a / 30 wt.% of $CaCO_3$ with treated and untreated surface are shown in Figure 3.10.

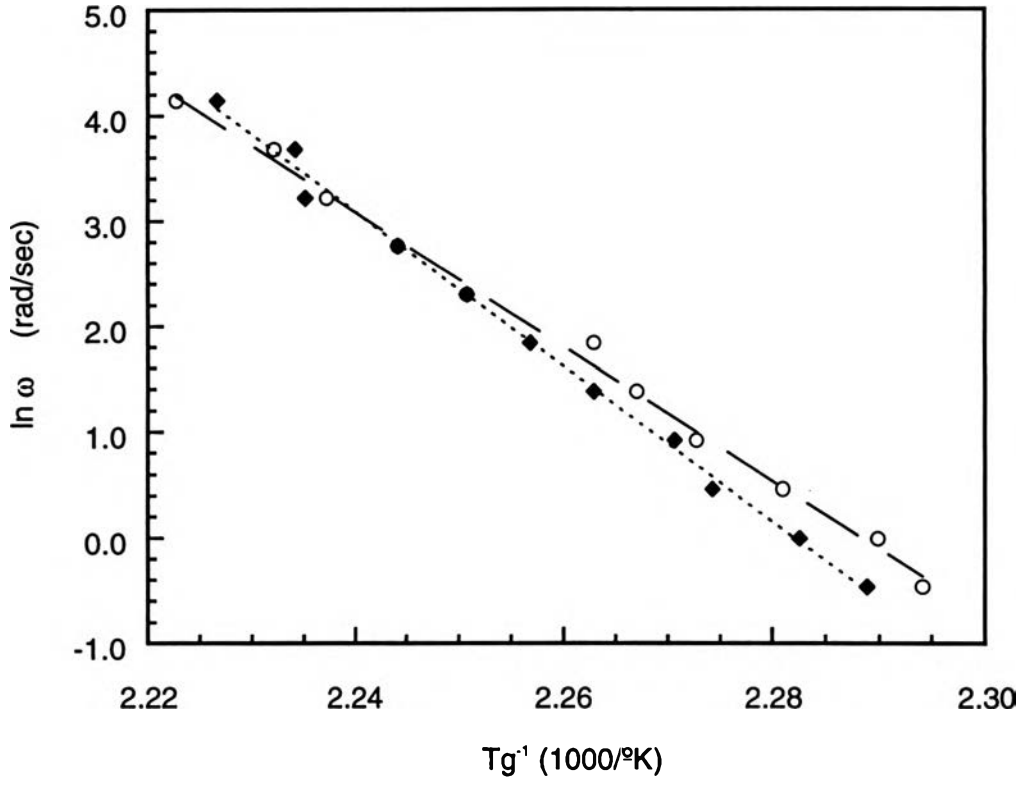

Figure 3.10 Arrhenius plot of logarithmic frequency versus inverse glass transition for B-a filled with surface treated (O) and untreated (◆) $CaCO_3$.

The ΔH calculated from these plots are 126 and 145 Kcal/mole for the B-a filled with surface treated and untreated $CaCO_3$, respectively. The higher ΔH of untreated $CaCO_3$, implies that the molecular motion at the glass transition process needs a higher energy to overcome the further restriction resulting from the better adhesion at the interface of untreated $CaCO_3$ and B-a (H. Ishida, 1993). The results from dynamic mechanical measurement can support the static mechanical testing.

3.5 Viscosity Measurement

The rheological understanding of a material is the most crucial factor in composite processing. Figure 3.11 shows plots of shear viscosity versus temperature for pure B-a monomer, the monomer with 18% oligomers, and phenolic oligomers of novolac type. Typically, a monomer or a small molecule shows an inverse relationship between the viscosity and temperature. However, the monomer starts to polymerize as the temperature increases. As a result, the characteristic of all curves display a dramatic drop of viscosity at the beginning temperature (80-110°C for B-a and 120-140°C for phenolic oligomers). Then the viscosity slightly declined at the elevated temperature. The viscosity of pure B-a monomer and the monomer with 18% oligomers are much lower than that of a novolac-type phenolic oligomers indicating that B-a offers a better opportunity for composite process design and manufacturing.

The plot of shear viscosity against temperature at different filler contents are displayed in Figure 3.12. The viscosity increases with increasing filler content and the characteristic of the curve does not change. It means that $CaCO_3$ does not have effect on kinetic of curing (does not act as catalyst or inhibitor), but only contributes restriction of mobility of monomer and oligomer molecules which are in contact with the $CaCO_3$ particle.

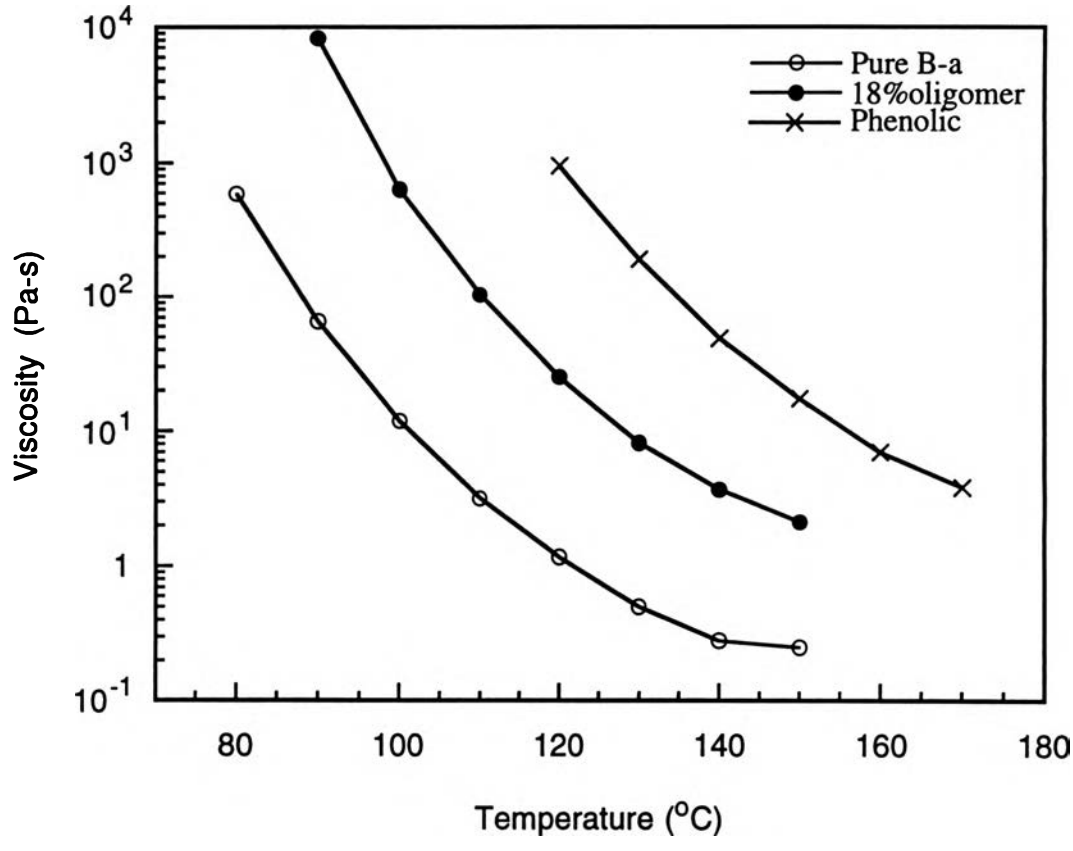

Figure 3.11 The plot of viscosity versus temperature of B-a monomer (O), 18% oligomers (●) and phenolic oligomer (×).

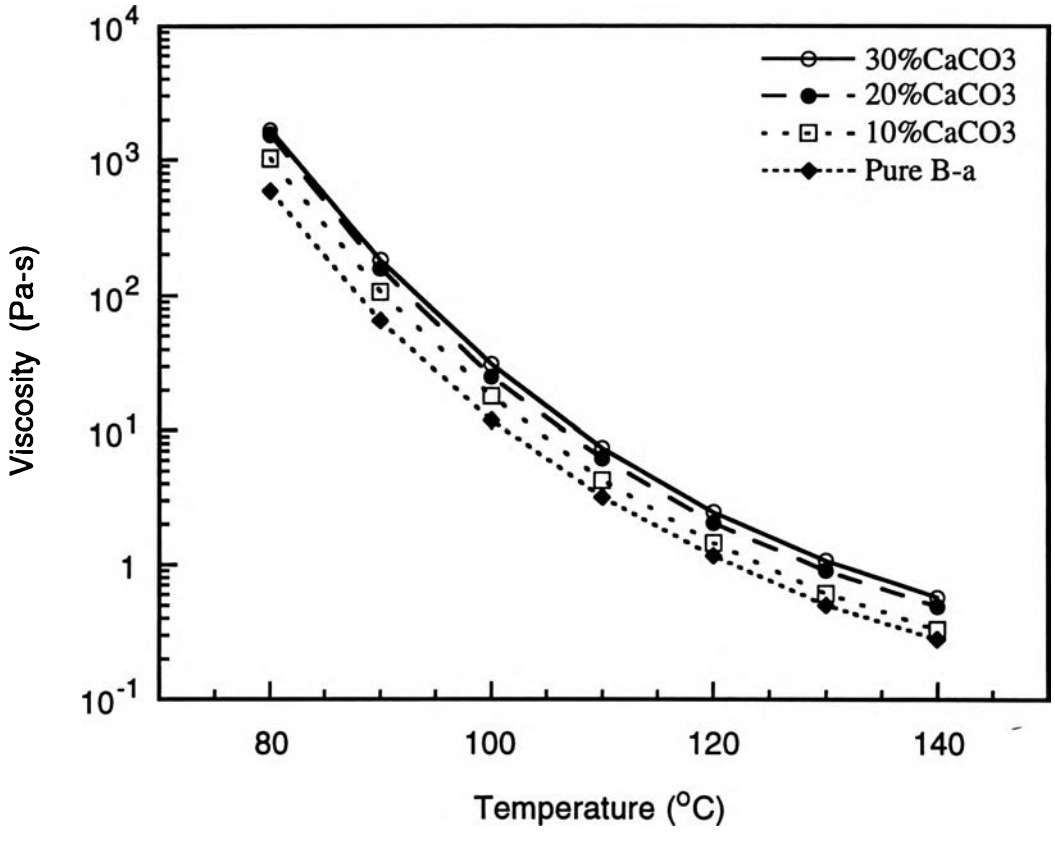

Figure 3.12 The plot of viscosity versus temperature of B-a filled with 0% (♦),10% (□), 20% (●) and 30% (O) $CaCO_3$.